Effect of Adding UV Absorbers Embedded in Carbonate Calcium Templates Covered with Light Responsive Polymer into a Clear Wood Coating

Caroline Queant * [ID], Pierre Blanchet, Véronic Landry and Diane Schorr

Department of Wood and Forest Sciences, Université Laval, Québec City, QC G1V 0A6, Canada; pierre.blanchet@sbf.ulaval.ca (P.B.); veronic.landry@sbf.ulaval.ca (V.L.); diane.schorr.1@ulaval.ca (D.S.)
* Correspondence: caroline.queant.1@ulaval.ca

Abstract: The limited durability of clear coatings is a major issue for the coating and wood industry. The addition of organic UV absorbers improves coating resistance by the absorption and the conversion of the UV radiation into harmless heat. Organic UVAs are prone to degradation and can migrate in the binder of coatings. In this study, commercial UVAs and HALS have been entrapped into $CaCO_3$ templates coated with stimuli responsive polymers. Microspheres were incorporated into a clear acrylic water-based coating formulation. The formulation was applied on glass and wood panels and was placed into an artificial UV chamber. This study presents a comparison between the aesthetic behavior of coating formulations with free and encapsulated commercial UVAs and HALS during the accelerated ageing test. Encapsulation of UVAs was confirmed by XPS and TGA analysis. Results have shown that the coating's aesthetic was slightly improved when using the encapsulated products.

Keywords: coatings; stimuli-sensitive polymers; structure-property relationships

1. Introduction

Wood used for exterior applications is prone to environmental damages such as photodegradation (UV). The most damaging radiations are between 290 and 350 nm. The Planck-Einstein relation $E = hc/\lambda$ (*E*: photon energy in joules; *c*: light speed in vacuum m/s; λ: wavelength in nm) states that the shorter the wavelength is, the higher the corresponding energy is. UV rays have enough energy to initiate scission reactions in polymer chains [1]. Lignin and carbohydrates components of wood are UV sensitive [2]. The resulting effect in wood leads to its discoloration and a change in its chemical and mechanical properties. The change in wood color is the first sign of chemical alteration [3–6].

To protect wood from alteration, coatings, impregnation, and chemical modification can be employed [7–9]. Applying coatings is the most common method to protect from degradation [10]. The desire amongst consumers for exterior clear coatings that will maintain the wood's appearance is expanding [11,12]. However, they are more sensitive to UV light than opaque coatings. Their transparency allows UV rays to reach the wood underneath [1,4,5].

The use of UV absorbers (UVAs) contributes to the UV protection of coatings by screening harmful radiations. Organic UVAs are molecules with conjugated π electrons systems that are able to absorb the UV radiation and convert it into harmless heat [13]. Benzophenones type UVAs are commonly used with HALS (hindered amine light stabilizers), which show synergistic photoprotection [14].

UV light responsive microspheres can be employed to release encapsulated materials upon UV illumination. An interesting group of molecules that can respond to near-UV and visible light are azobenzenes. Azobenzene molecules contain two phenyl groups attached by a N=N bond.

This bond allows a cis-trans rearrangement by UV absorption [15]. Microspheres are used in various applications [16,17]. Studies from Yi et al. (2014) [18] have shown synthesis of UV responsive polyelectrolyte microcapsules by sequential deposition. With UV exposure, microcapsules were disrupted. This has the effect to modulate protein release. Zhao et al. (2012) [19] worked on the design and preparation of light-responsive biocompatible micelles. Applications are light triggering delivery of drugs and others bioagents. Microspheres have been introduced into coatings in many studies and applications.

The main objective of this study is to suggest a tailored solution to increase the durability of clear coatings. In this study, encapsulation of organic UVAs in microspheres is used for UV protection improvement. Poly(1-(4-(3-carboxy-4-hydroxyphenyl-azo)benzenesulfonamido)-1,2-ethanediyl) (PAZO) is used as a light responsive polymer. UVAs and HALS were encapsulated into $CaCO_3$ templates with PAZO and poly(diallyldimethylammonium chloride) (PDADMAC) layers. Encapsulated compounds were incorporated into water-based acrylic coating formulations. Artificial accelerated weathering was performed to evaluate the effect of encapsulated compounds on the behavior of coating aesthetic in response to intense UV exposition.

2. Materials and Methods

2.1. Materials

1-propanol, $CaCl_2$, Na_2CO_3 (Fisher Chemical, St Louis, MO, USA), poly(diallyldimethylammonium chloride) solution (PDADMAC M_w 200,000–350,000, 20 wt.% in H_2O), and poly(1-(4-(3-carboxy-4-hydroxyphenyl-azo)benzenesulfonamido)-1,2-ethanediyl, sodium salt) (PAZO) (Figure 1) (Sigma Aldrich, St Louis, MO, USA) were used without any further purification. UV stabilizers Tinuvin 1130 and Tinuvin 292 (derived from tetramethyl piperidine) were obtained from BASF (Laval, QC, Canada). The commercial UVA used in this study is of the hydroxyphenylbenzotriazole type (Figure 2). Deionized water was used throughout this study.
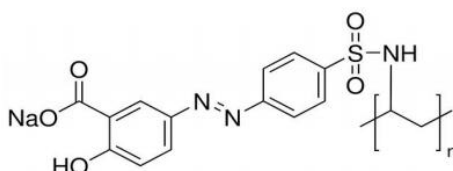

Figure 1. Chemical structure of the poly(1-(4-(3-carboxy-4-hydroxyphenylazo)benzenesulfonamido)-1,2-ethanediyl) (PAZO) polymer.
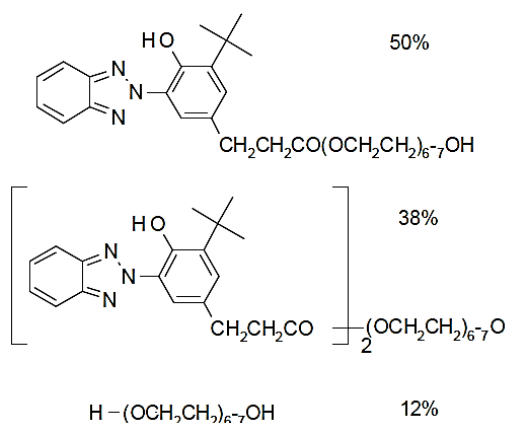

Figure 2. Chemical composition of Tinuvin 1130.

2.2. Synthesis of CaCO$_3$ Templates with Tinuvin 1130 and Tinuvin 292

The formation of CaCO$_3$ templates with embedded Tinuvin 1130 and Tinuvin 292 was obtained by the coprecipitation (Figure 3) of CaCl$_2$ and Na$_2$CO$_3$ salts [20]. CaCO$_3$ templates were prepared by mixing equal volume of Na$_2$CO$_3$ (1 M) and CaCl$_2$ (1 M) solutions under magnetic stirring for 1 h. 0.1 g of concentrated commercial solution of Tinuvin 1130 or Tinuvin 292 was added to the CaCl$_2$ solution prior to the mixing with the Na$_2$CO$_3$ solution. During the precipitation process, the precipitates were vigorously stirred by a magnetic stirring bar. They were then rinsed three times with deionized water. After removing the supernatant, the precipitates were dried at 80 °C for 2 days and stored at room temperature prior to use.

To obtain complete dissolution of Tinuvin 1130 and Tinuvin 292, 40 wt.% of the water was replaced by 1-propanol into the CaCl$_2$ solution.
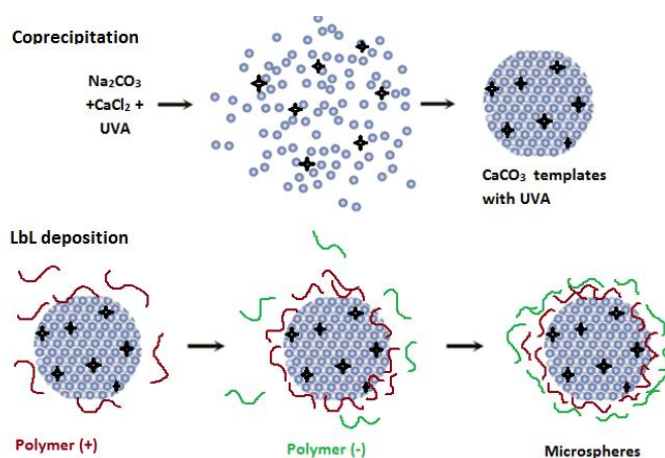

Figure 3. Synthesis of CaCO$_3$ templates and layer by layer deposition.

2.3. Layer by Layer Deposition of Polyelectrolytes

Polyelectrolytes were deposited on the CaCO$_3$ templates alternately for 15 min (Figure 3), starting with the positively charged PDADMAC (1 mg/mL in 0.15 M NaCl) and then the negatively charged PAZO (1 mg/mL in 0.15 M NaCl). Resulting coated microspheres were washed three times with purified water. To avoid aggregation, microspheres were ultrasonicated for 10 s after each deposition step. The layer by layer deposition technique was already used in several studies for polyelectrolyte deposition and coating of various inorganic microspheres [15,21,22].

3. Characterization Techniques

Transmission Electron Microscopy (TEM) was performed on the microspheres to investigate the shape. The observation was performed by using an electronic microscope JOEL 1230 (Peabody, MA, USA) at an acceleration voltage of 80 kV. Microsphere solutions were directly deposited on nickel microscope grids coated with carbon and formvar.

3.1. XPS

X-ray photoelectron spectroscopy (XPS) was used to study the chemical composition of the 10 nm surface of grinded CaCO$_3$ templates with commercial UVAs. Experiments were performed with an XPS instrument (Axis-Ultra) from Kratos Analytical, Manchester, UK. This equipment is composed of three communicating chambers: the analysis chamber comprising the ESCA analyzer, the preparation chamber, and the introduction chamber. Survey scans were recorded using an X-ray monochromatic Al source operated at 300 W. The X-ray source was oriented with a 30° incidence angle. Scans were obtained with pass energy of 160 eV and with lens used in hybrid mode. Survey scans were used for

elemental analysis and apparent concentration calculations. Calculation of the apparent relative atomic concentrations were performed with the software CasaXPS (Version 2.1.9, 2002) based on principles found in standard textbooks and using sensitivity factors pertinent to the operating conditions of the spectrometer.

3.2. TGA

Thermogravimetric analysis curves were collected with a thermoanalyzer TGA 851e from Mettler Toledo (Columbus, OH, USA). Measurements were performed over a 25–850°C temperature range at 10 °C/min under a nitrogen flow. Crucibles used were made of aluminum oxide. Three replicates were performed for each sample.

3.3. Introduction of Encapsulated UVAs in an Acrylic Water-Based Formulation

Microspheres were pre-dispersed in water in order to obtain a better distribution before the addition to the paint formulation (Table 1). Percentages of UVAs and HALS added to the formulation are detailed in Table 2. The solution was mixed with a given paint formulation using a high-speed disperser Dispermat LC 30 (BASF) at 1000 rpm for 1 h. Several formulations were prepared and applied on glass and wood panels for testing (Table 2). The control sample contained only the paint formulation without any protective absorber.

Table 1. Clear coat complete formulation.

Formulation	Weight (g)
Acrylic binder	50.23
Water	30.9
Solvent and plasticizer	1.68
Liquid rheological	1.6
Silicone surfactant	0.71
Defoamer	0.56
Biocide	0.05

Table 2. Composition of the formulations.

Sample	Free UVAs (wt.%)	Free HALS (wt.%)	$CaCO_3$ + UVAs (wt.%)	$CaCO_3$ + HALS (wt.%)
Control	–	–	–	–
Formulation 1	0.1	–	–	–
Formulation 2	0.1	0.1	–	–
Formulation 3	–	–	2.5	–
Formulation 4	–	–	2.5	2.5

UVAs and hindered amine light stabilizers (HALS) are often utilized together to improve their performance. Tinuvin 1130 (UVA) and Tinuvin 292 (HALS) are indeed known to have a synergistic effect [23,24]. Part of the formulations were prepared using UVAs as well as HALS.

For an optimal protection, BASF guidelines advise the use of 1–3 wt.% of UVA and 0.5–2 wt.% of HALS, which explains the UVA concentration selected. Concentrations are based on weight percent binder solids. All formulations were prepared in triplicates.

3.4. Weathering Tests

Two types of accelerated artificial ageing tests devices were used—Atlas Ci3000 + Weather-Ometer (Atlas Electric Devices Company, Mount Prospect, IL, USA) and a QUV accelerated weathering tester from Q-Lab (Westlake, OH, USA). To evaluate the coating behavior on its own, tests were first carried on glass supports of 68 mm × 144 mm × 4 mm. Samples were exposed to a xenon lamp of 4500 W in the Weather-Ometer. Artificial xenon exposures were performed to simulate the entire UV and visible

spectrum of daylight. The filter combination used was an inner Type S Boro and an outer Soda Lime. Samples were exposed to 2500 h of ageing. The standard test method employed for accelerated ageing tests is the ASTM G155 "Standard Practice for Operating Xenon Arc Light Apparatus for Exposure of Non-Metallic Materials" [25]. Cycle 4 was selected: the irradiance was set at 0.30 W m^{-2} nm^{-1} with 100% light, 55% relative humidity, at 55 °C black panel temperature. No water spray was used. This cycle was chosen because the continuous lightening could induce quicker degradation.

The second series of tests was performed on wood panels. White spruce (*Picea glauca* (Moench) Voss) boards were obtained from Maibec (Saint-Pamphile, QC, Canada) and were cut into 75 mm × 50 mm × 4 mm samples. They were sanded with P150 sand paper after being stored and conditioned at 20 °C and 65% relative humidity until constant mass at 12% humidity. Panels were placed into the accelerated ageing tester QUV. Tests were performed in accordance to the ASTM G154-2012 Standard test method "Standard Practice for operating Fluorescent Ultraviolet (UV) Lamp Apparatus for exposure of non-metallic Materials" [26]. Cycle 1 was selected. The first step is at a temperature of 60 °C and energy 0.89 W/m^2 for 8 h. The condensation cycle then begins at 50 °C Black Panel Temperature for 4 h. An UV-A 340 lamp (Q-Lab, Westlake, OH, USA) was used for the irradiation at 0.89 W m^{-2} nm^{-1} to simulate the UV portion of the solar spectrum. This cycle was chosen with a dark phase to reproduce more precisely the natural light cycle.

Formulations were applied on glass substrate and wood panels with a roller-coater (BYK, Wesel, Germany) at a speed of 50 mm/s. Two wet layers of 50 µm of each coating were deposited.

3.5. Colorimeter

The color change in the coating systems was measured with a colorimeter (BYK-Gardner Colorguide 45/0, Wessel, Germany). Three measurements were taken for each sample. The average value was calculated and is reported in this paper. CIELAB (defined by the International Commission on Illumination (CIE) *L**a*b*. *L** for the lightness and *a** and *b** for the green–red and blue–yellow color components) color scale was used. Three coordinates (*L**, *a**, and *b**) were determined for each sample. Chromatic coordinates are *L**, which is the lightness from black (0) to black/white (100); *a**, the color component from green (−60) to red (+60); and *b**, the color component from blue (−60) to yellow (+60). Each component's evolution was evaluated separately [10].

4. Results and Discussion

4.1. Characterization Techniques

CaCO$_3$ microspheres coated with polyelectrolytes were observed with TEM at 400×. Images (Figure 4) show microspheres of sizes ranging from approximatively 10 nm to 300 nm. Size distribution was found to be highly heterogeneous. The morphology observed is mostly polygonal, while some particles are cubic.
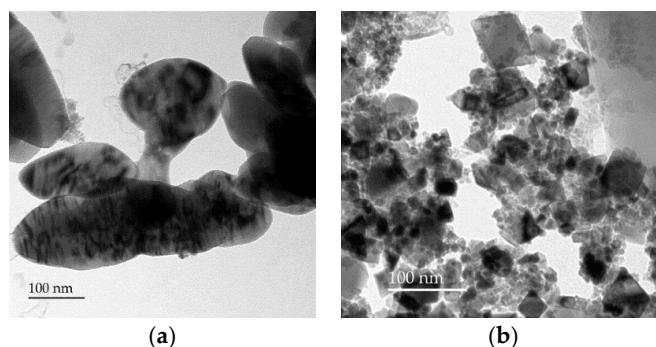

(**a**)	(**b**)

Figure 4. Observation of CaCO$_3$ coated microspheres with Transmission Electron Microscopy (TEM) 400×: (**a**) Agglomeration of CaCO$_3$ microspheres; (**b**) Cubic CaCO$_3$ coated particles.

4.2. XPS

Apparent relative concentrations are given by atomic percentages on survey spectra. Hydrogen is not included as it is not detectable. Concentrations are apparent and considered homogeneous on the entire volume analyzed (800 μm × 400 μm × 5 nm). The survey spectrum (Figure 5) shows atomic composition quantity for carbon, nitrogen, calcium, sodium, oxygen, chlorine, and phosphorus elements. Phosphorous could come from the water medium of the coprecipitation reaction.
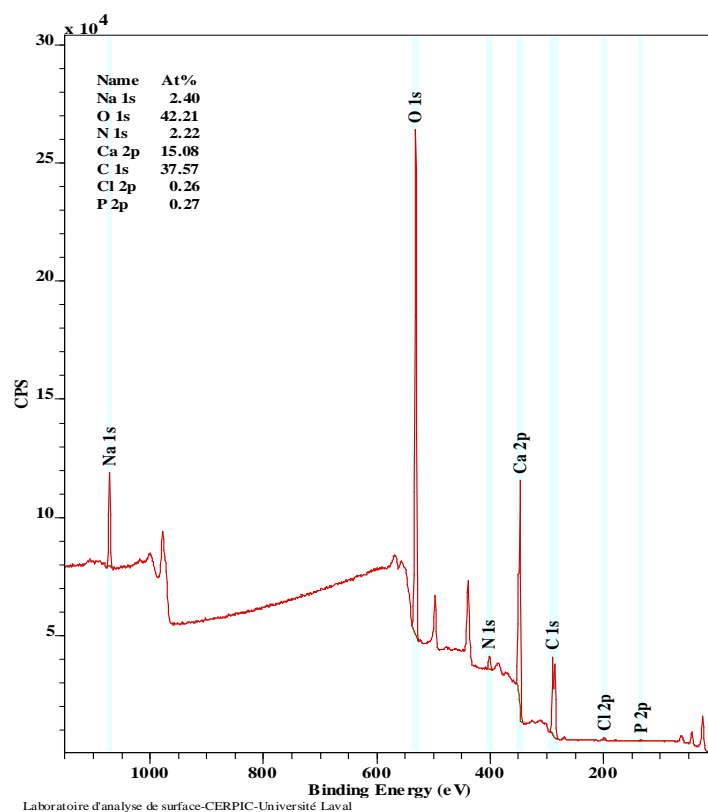
Name	At%
Na 1s	2.40
O 1s	42.21
N 1s	2.22
Ca 2p	15.08
C 1s	37.57
Cl 2p	0.26
P 2p	0.27

Laboratoire d'analyse de surface-CERPIC-Université Laval

Figure 5. Survey spectrum of elementary analysis on embedded UVAs into $CaCO_3$ sample.

The Ca spectrum (Figure 6) shows a Ca 2*p* characteristic peak of a carbonate. This is also confirmed by the C 1*s* spectrum (Figure 7). The binding energy of 289.51 eV corresponds to an O=C–O group, which is also characteristic of a carbonate. These elements show that the coprecipitation process has correctly happened. It has led to the formation of carbonates such as $CaCO_3$ [27].

N 1*s* high resolution spectrum (Figure 8) shows two narrow peaks of different binding energies and another large peak that can correspond to a nitrogen atom linked to an aromatic carbon. N 1*s*-1 peak binding energy corresponds to a pyrrole or pyridone group [28]. N 1*s*-2 peak corresponds to a C_{arom}–N–X. These two groups belong to the Tinuvin 1130 molecule. This result shows that Tinuvin 1130 is embedded into the $CaCO_3$ templates.
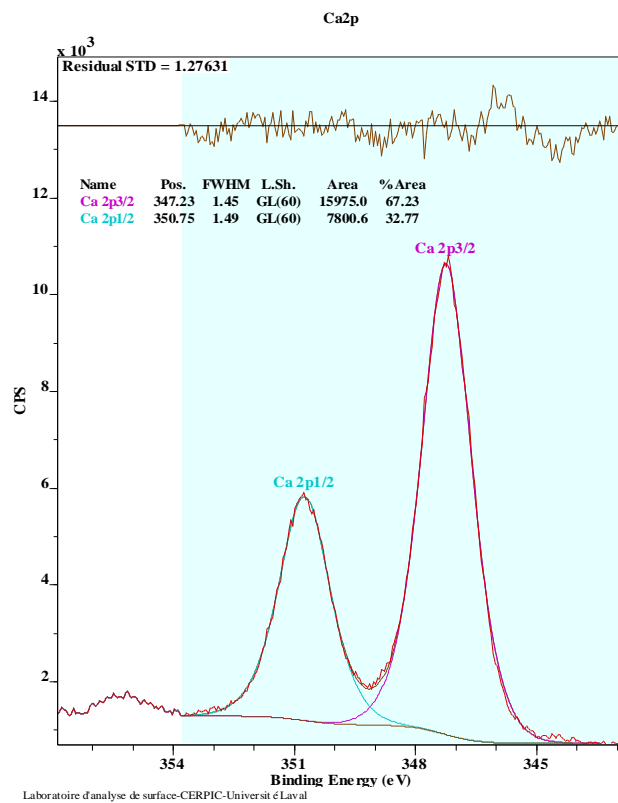
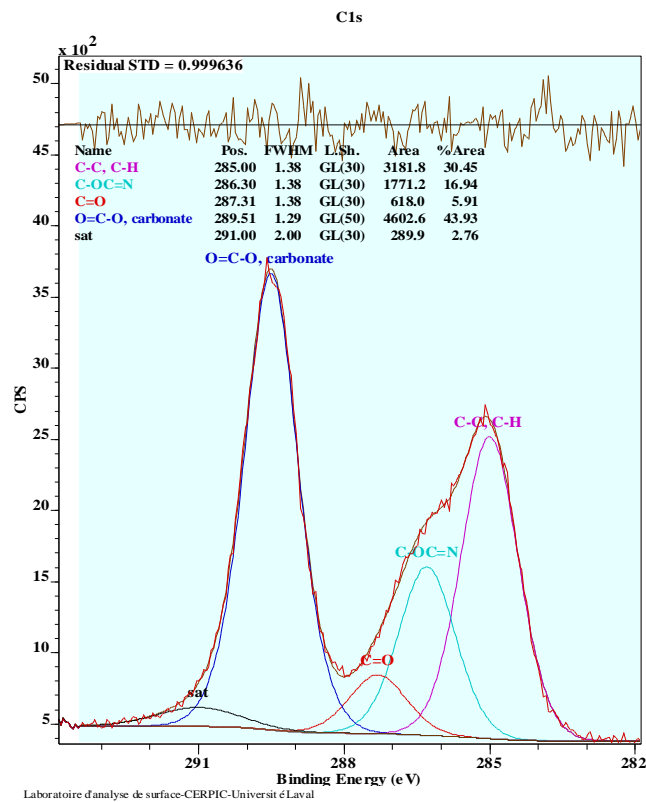**Figure 6.** Ca 2*p* high resolution spectra on embedded UVAs into CaCO₃ sample.

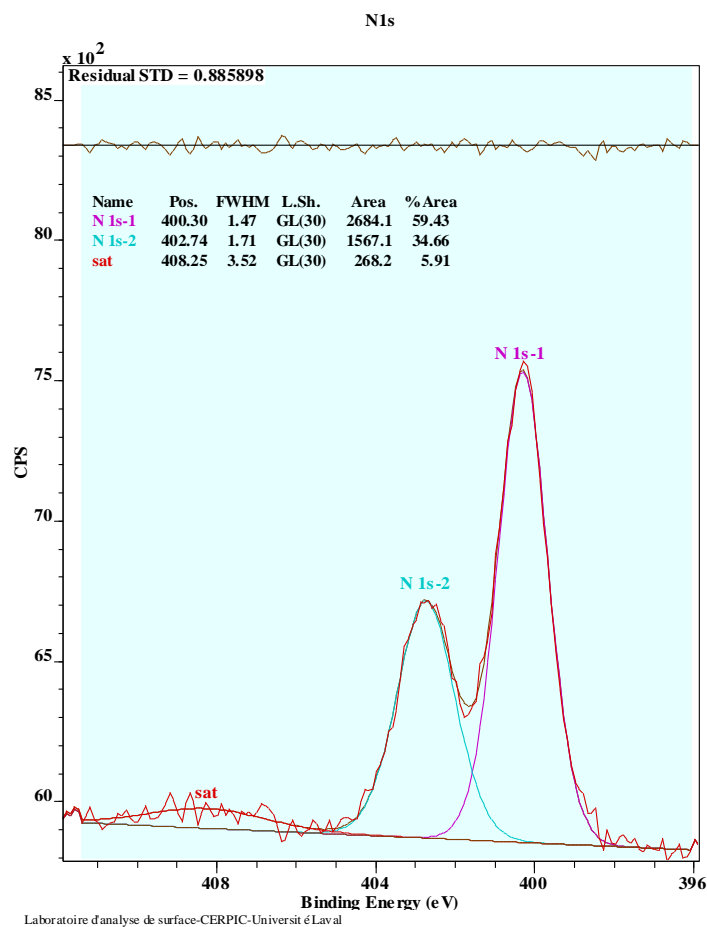**Figure 7.** C 1*s* high resolution spectra on embedded UVAs into CaCO₃ sample.

Figure 8. N 1*s* high resolution spectra on embedded UVAs into CaCO$_3$ sample.

4.3. TGA

Control CaCO$_3$ templates (Figure 9) start degrading at 700 °C. Under nitrogen, 84.5% ($\pm$1.6) of the CaCO$_3$ template alone is thermally degraded at the end of the analysis at 900 °C. A CaCO$_3$ sample with embedded UVAs was also analyzed. The weight loss at 900 °C was 78.6% ($\pm$1.9) for this sample. UVAs start to degrade from 200 to 600 °C. Entrapped UVAs take more time to evaporate and degrade. The weight loss difference between CaCO$_3$ samples with and without UVAs corresponds to the evaporation and degradation of the embedded UVAs. Coated CaCO$_3$ templates present a different thermoanalysis because of the degradation of the polyelectrolytes. It starts at approximatively 100 °C and goes up to 850 °C or even more. The thermal degradation of azo polymers and azo organic molecules was studied in [29]. Five percent weight loss temperature of azo polymers was found to be between 274 and 302 °C. Those temperatures correspond to the degradation found in this study. Along with the polyelectrolytes degradation, CaCO$_3$ begins to degrade at 700 °C.
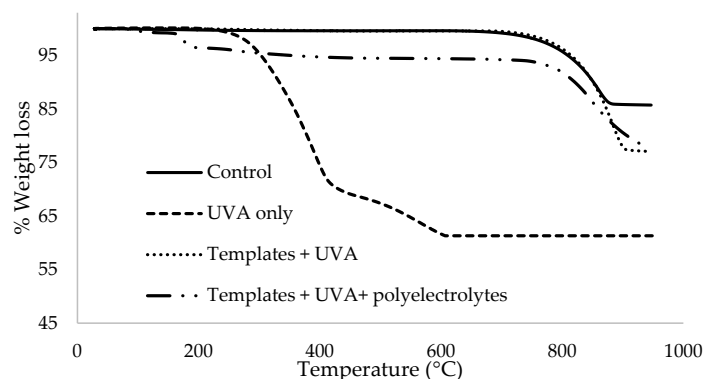
Figure 9. Thermoanalysis curves of samples of control, UVAs only, $CaCO_3$ templates + UVAs, and on $CaCO_3$ templates with UVAs and polyelectrolytes.

4.4. Weathering Tests

Monitoring the color of wood and its coatings allows to obtain information on coating degradation. An efficient coating should help to keep a stable color. The overall color variation (ΔE) should tend to zero (Figure 10) [10]. Color is measured as a function of exposure time. In this study, the overall color varies more for the encapsulated formulations. Because ΔE is only a vector, it is important to dissociate and study the color components evolution.

Figure 10. Evolution of ΔE for the different formulations on glass panels with Weather-Ometer exposure.

The monitoring of the separate components (a^*, b^*, and L^*) shows more precise information in the variation. The evolution of a^* and b^* (Figure 11) shows a different behavior for the encapsulated formulations. Non-encapsulated formulations remain stable after 600 h of Weather-Ometer exposition. Encapsulated formulations evolve toward blue ($-$) and red ($+$). This transition could be explained by the conformational change of the PAZO molecule. The photoisomerization reaction of azobenzene groups is triggered by UV irradiation (Figure 12) [21]. Two separate absorption regions are responsible for the trans-cis and cis-trans isomerization of the azobenzene molecules. Once the transition of molecular conformation is achieved, the absorbance changes, and therefore the color shifts [30]. This transition is also well visible in photos before and after weathering (Figure 13). The formulation with non-encapsulated UVAs have clearly photoyellowed, which is not the case of the encapsulated UVAs formulations. The encapsulated formulations have prevented coatings to yellow.
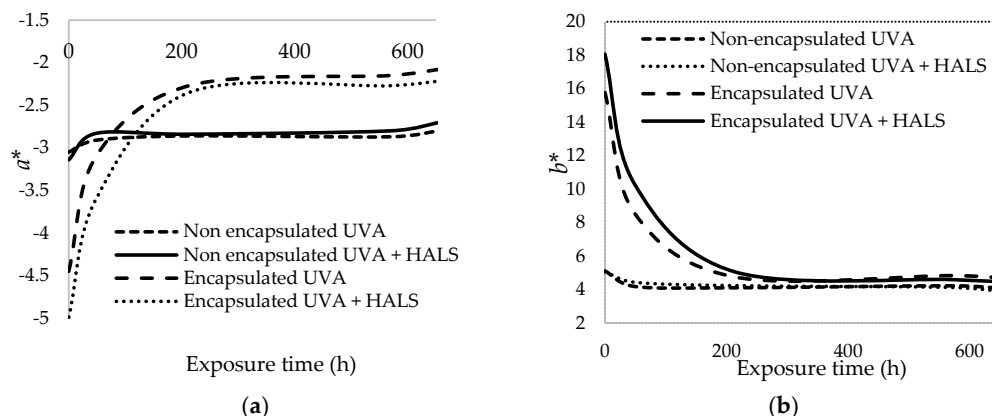
Figure 11. Evolution of (**a**) *a**and (**b**) *b** for the different formulations on glass panels with Weather-Ometer exposure.
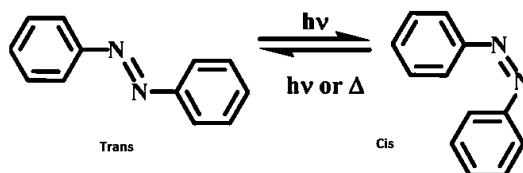

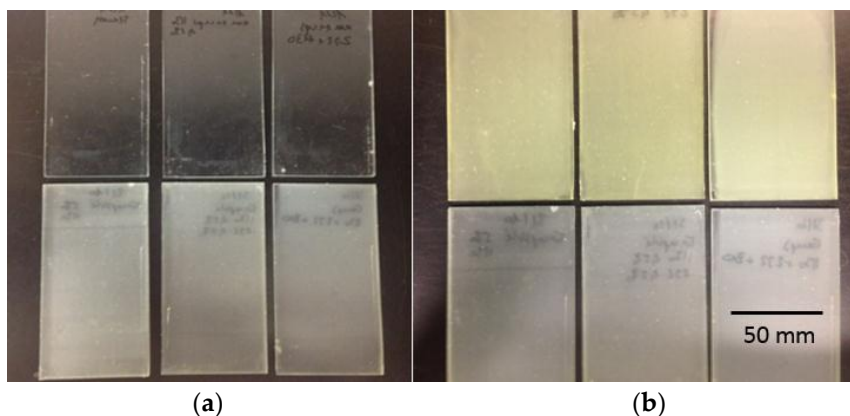**Figure 12.** Photoisomerization reaction of PAZO molecule. Adapted from [30].

Figure 13. Photos before (**a**) and after (**b**) weathering of the non-encapsulated formulations on glass support of 68 mm × 144 mm × 4 mm (top) and the encapsulated ones (bottom).

Formulations were applied on white spruce panels to test the behavior of wood underneath the formulations. After only 48 h of exposure in QUV tester, some formulations as well as the control sample start to darken. Wood color depends on UV protection efficiency. Changes in wood color reflect chemical degradation occurring during weathering [3]. Photoinduced discoloration starts to occur after only 24 h of QUV exposure. This phenomenon is explained by the lignin degradation and the formation of unsaturated aromatic compounds [10]. The test was carried out for 2500 h.

The color monitoring of the wood panels allows to study wood degradation and thus UV protection efficiency. The most efficient protective coating should absorb the entire UV spectrum, and thus no UV light should reach the wood underneath. Wood discoloration is a sign of wood degradation and of a less efficient coating.

For *L** color components (Figure 14) all formulations show the most important color variation in the first 500 h of exposure. This early phenomenon is caused by the visible radiation, which

decomposes yellowing products into colorless compounds [31]. This effect is worse with accelerated testing devices at high light intensity and with shorter dark periods than in natural exposition [32]. Light sources emitting fluorescent UV-A tubes induce exaggerated and unnatural photoyellowing [33]. This change in color at the beginning has no impact on mechanical properties of the binder [31,33]. The change affects only the aesthetic properties of the wood.

For the formulations with encapsulated compounds, the *L** parameter (Figure 14) presents a good stability from 500 to 2500 h of QUV exposition for encapsulated formulations. The slope of the curve for the formulations with non-encapsulated UVAs is slightly more pronounced, which shows that the wood is still darkening during UV exposition. The parameter *a** (Figure 15) during UV exposition evolves toward red and then reaches stabilization after 500 h. The formulation with non-encapsulated UVAs and HALS presents a slope near 0, which makes the best formulation for the *a** component only. The evolution of the *b** component (Figure 16) shows a similar slope for the different formulations. However, the yellowing is minimized with encapsulated compounds (lower *b** values).
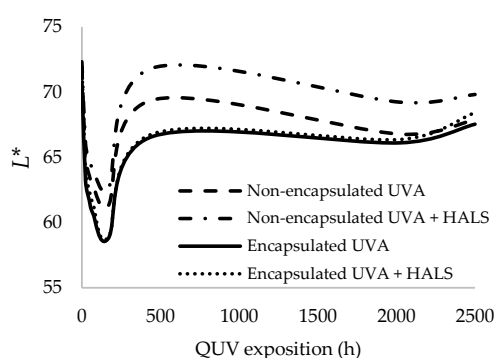

Figure 14. *L** component evolution for the different formulations studied with QUV exposure.
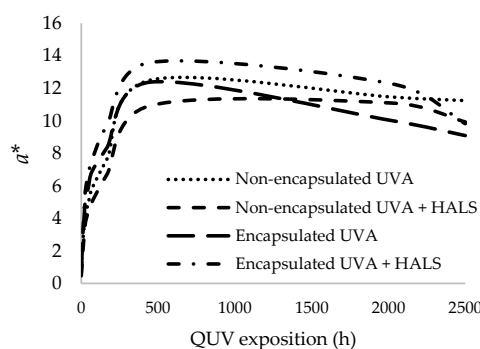

Figure 15. *a** component evolution for the different formulations studied with QUV exposure.
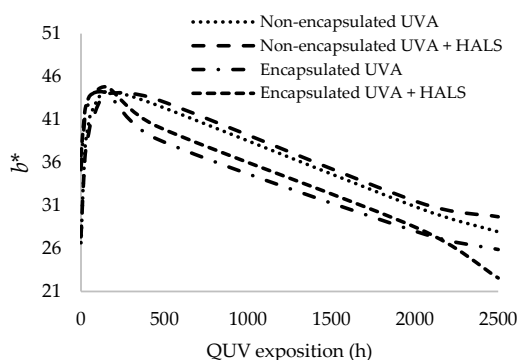

Figure 16. *b** component evolution for the different formulations studied with QUV exposure.

In comparison to formulations with non-encapsulated compounds, formulations with encapsulated compounds were found to be slightly more stable. Indeed, darkening and yellowing evolve more slowly during the UV illumination. One explanation is that the PAZO rearrangement observed on glass support causes the small evolution of color.

5. Conclusion

Very few studies report the preparation and the use of UV responsive microspheres. The main objective of the study was to examine the effect of adding microspheres in a transparent acrylic water-based formulation. Commercial UVAs and HALS were embedded into $CaCO_3$ templates by coprecipitation of $CaCl_2$ and Na_2CO_3. Polyelectrolytes were deposited around the templates. PAZO is a light responsive polymer which changes its polymer structure upon radiation. The synthesis method was found to be efficient to encapsulate a small amount of UVAs and HALS. Microspheres prepared were incorporated into a clear coat formulation.

Colorimetric studies on glass support show proof of the molecular transition in conformation of PAZO chains. This transition is revealed by a modification of the absorption during UV exposition. Experiments on wood panels show a similar behavior for formulations with non-encapsulated and encapsulated compounds. Color analysis reveals a global color evolution toward red, blue, and black. Although it is difficult to extrapolate about UV protection efficiency from color results, encapsulated formulations appear to prevent darkening from yellowing. One solution to improve efficiency of encapsulated formulations would be to achieve a better encapsulation of UVAs and HALS. This could be done by optimizing the coprecipitation process and solubility of products.

These conclusions are exploratory results meant to assess the effect of adding encapsulated UVAs into a clear coat formulation. Encapsulated UVAs could give an alternative solution in the field of clear coat UV protection. Encapsulated UVAs could help to preserve wood aesthetics and provide more durable protection.

These data only show aesthetic and colorimetric analysis. Future studies should include results on mechanical and physical properties. Results obtained in the present study are from an accelerated weathering tester. Further studies should include natural exposition data.

References

1. Williams, R.S. Weathering of wood. In *Handbook of Wood Chemistry and Wood Composites*; Rowell, R.M., Ed.; CRC Press: Boca Raton, FL, USA, 2005; Volume 7, pp. 139–185.
2. Saha, S.; Kocaefe, D.; Sarkar, D.K.; Boluk, Y.; Pichette, A. Effect of TiO_2-containing nano-coatings on the color protection of heat-treated jack pine. *J. Coat. Technol. Res.* **2010**, *8*, 183–190. [CrossRef]
3. Nikolic, M.; Lawther, J.M.; Sanadi, A.R. Use of nanofillers in wood coatings: A scientific review. *J. Coat. Technol. Res.* **2015**, *12*, 445–461. [CrossRef]
4. Evans, P.D. Weathering and Photoprotection of Wood. In *Development of Commercial Wood Preservatives*; ACS Symposium Series; Schultz, T.P., Militz, H., Freeman, M.H., Goodell, B., Nicholas, D.D., Eds.; University of British Columbia: Vancouver, BC, Canada, 2008; pp. 69–117.
5. Nejad, M.; Cooper, P. Exterior wood coatings. In *Wood in Civil Engineering*; Concu, G., Ed.; InTech: London, UK, 2017.

6. Rowell, R.; Bongers, F. Coating acetylated wood. *Coatings* **2015**, *5*, 792–801. [CrossRef]

7. Black, J.M.; Mraz, E.A. *Inorganic Surface Treatments for Weather Resistant Natural Finishes*; U.S. Department of Agriculture, Forest Service: Madison, WI, USA, 1974; p. 40.

8. Feist, W.C. *The Role of Water Repellents and Chemicals in Controlling Mildew on Wood Exposed Outdoors*; U.S. Department of Agriculture, Forest Service: Madison, WI, USA, 1984; p. 16.

9. Evans, P.D.; Owens, N.L.; Schmid, S.; Webster, R.D. Weathering and Photostability of Benzoylated Wood. *Polym. Degrad. Stab.* **2002**, *76*, 291–303. [CrossRef]

10. Auclair, N.; Riedl, B.; Blanchard, V.; Blanchet, P. Improvement of Photoprotection of Wood Coatings by Using Inorganic Nanoparticles as UV Absorbers. *For. Prod. J.* **2011**, *61*, 20–27.

11. Evans, P.D.; Haase, J.G.; Seman, A.S.; Kiguchi, M. The search for durable exterior clear coatings for wood. *Coatings* **2015**, *5*, 830–864. [CrossRef]

12. Collins, P. Woodcare (interior and exterior architectural coatings): Market statistics and technology development. In Proceedings of the PRA's 9th International Woodcoatings Congress, Amsterdam, The Netherlands, 14–15 October 2014.

13. Fajzulin, I.; Zhu, X.; Möller, M. Nanoparticulate inorganic UV absorbers: A review. *J. Coat. Technol. Res.* **2015**, *12*, 617–632. [CrossRef]

14. Pickett, J.E. Permanence of UV absorbers in plastics and coatings. In *Handbook of Polymer Degradation*; Halim, H.S., Ed.; CRC Press: Boca Raton, FL, USA, 2000; p. 163.

15. Bedard, M.F.; De Geest, B.G.; Skirtach, A.G.; Mohwald, H.; Sukhorukov, G.B. Polymeric microcapsules with light responsive properties for encapsulation and release. *Adv. Colloid. Interface Sci.* **2010**, *158*, 2–14. [CrossRef] [PubMed]

16. Hebert, M.L.; Shah, D.S.; Blake, P.; Servoss, S.L. Uniform and robust peptoid microsphere coatings. *Coatings* **2013**, *3*, 98–107. [CrossRef]

17. Jenkins, J.S.; Flickinger, M.C.; Velev, O.D. Continuous convective-sedimentation assembly of colloidal microsphere coatings for biotechnology applications. *Coatings* **2013**, *3*, 26–48. [CrossRef]

18. Yi, Q.; Sukhorukov, G.B. UV-induced disruption of microcapsules with azobenzene groups. *Soft Matter* **2014**, *10*, 1384–1391. [CrossRef] [PubMed]

19. Zhao, Y. Light-responsive block copolymer micelles. *Macromolecules* **2012**, *45*, 3647–3657. [CrossRef]

20. Hua, B.; Deng, B.; Thornton, E.C.; Yang, J.; Amonette, J.E. Incorporation of chromate into calcium carbonate structure during coprecipitation. *Water Air Soil Pollut.* **2006**, *179*, 381–390. [CrossRef]

21. Han, J.; Yan, D.; Shi, W.; Ma, J.; Hong, Y.; Wei, M.; Evans, D.G.; Duan, X. Layer-by-layer ultrathin films of azobenzene-containing polymer/layered double hydroxides with reversible photoresponsive behavior. *J. Phys. Chem. B* **2010**, *114*, 5678–5685. [CrossRef] [PubMed]

22. Caruso, F. Hollow capsule processing through colloidal templating and self-assembly. *Chem. Eur. J.* **2000**, *6*, 413–419. [CrossRef]

23. Shenoy, M.A.; Marathe, Y.D. Studies on synergistic effect of UV absorbers and hindered amine light stabilisers. *Pigment Resin Technol.* **2007**, *36*, 83–89. [CrossRef]

24. Schaller, C.; Rogez, D.; Braig, A. Hindered amine light stabilizers in pigmented coatings. *J. Coat. Technol. Res.* **2008**, *6*, 81–88. [CrossRef]

25. *ASTM-G155 Standard Practice for Operating Xenon Arc Light Apparatus for Exposure of Non-Metallic Materials*; ASTM International: West Conshohocken, PA, USA, 2005.

26. *ASTM G154-2012 Standard Practice for Operating Fluorescent Ultraviolet (UV) Lamp Apparatus for Exposure of Nonmetallic Materials*; ASTM International: West Conshohocken, PA, USA, 2012.

27. Moulder, J.F.; Stickle, W.F.; Sobol, P.E.; Bomben, K.D. *Handbook of X-ray Photoelectron Spectroscopy*; Chastain, J., Ed.; Physical Electronics Desivion, Perkin-Elmer Corporation: Eden Prairie, MN, USA, 1995; pp. 230–232.

28. Raymundo-Pinero, E.; Cazorla-Amoros, D.; Linares-Solano, A.; Find, J.; Wild, U.; Schlogl, R. Structural characterization of n-containing activated carbon fibers prepared from a low softening point petroleum pitch and a melamine resin. *Carbon* **2002**, *40*, 597–608. [CrossRef]

29. Ye, F.; Gu, P.; Zhou, F.; Liu, H.; Xu, X.; Li, H.; Xu, Q.; Lu, J. Preparation of homopolymers from new azobenzene organic molecules with different terminal groups and study of their nonvolatile memory effects. *Polymer* **2013**, *54*, 3324–3333. [CrossRef]

30. Bédard, M.; Skirtach, A.G.; Sukhorukov, G.B. Optically driven encapsulation using novel polymeric hollow shells containing an azobenzene polymer. *Macromol. Rapid Commun.* **2007**, *28*, 1517–1521. [CrossRef]

31. Lemaire, J. Predicting polymer durability. *Chemtech* **1996**, *26*, 42–47.

32. Pickett, J.E. Reversible post-exposure yellowing of weathered polymers. *Polym. Degrad. Stab.* **2004**, *85*, 681–687. [CrossRef]

33. Haillant, O. Accelerated weathering testing principles to estimate the service life of organic PV modules. *Sol. Energy Mater. Sol. Cells* **2011**, *95*, 1284–1292. [CrossRef]